



Selective inducible microsomal prostaglandin E₂ synthase-1 (mPGES-1) inhibitors derived from an oxacam template

Jane Wang^{a,*}, David Limburg^a, Jeff Carter^b, Gabriel Mbalaviele^a, James Gierse^a, Michael Vazquez^a

^a Pfizer Inc. St. Louis Laboratory, PG RD Research, 700 Chesterfield PKWY W, Chesterfield, MO 63017, USA

^b IcaGen, Inc. 4222 Emperor Blvd., Suite 350 Durham, NC 27703, USA

ARTICLE INFO

Article history:

Received 19 November 2009

Revised 11 January 2010

Accepted 13 January 2010

Available online 25 January 2010

ABSTRACT

Here we describe the SAR of a series of potent and selective mPGES-1 inhibitors based on an oxacam template. Compound **13j** demonstrated low nanomolar mPGES-1 inhibition in an enzyme assay. In addition, it displayed PGE₂ inhibition in a cell-based assay (0.42 μM) and had over 238-fold selectivity for mPGES-1 over COX-2 and over 200-fold selectivity for mPGES-1 over 6-keto PGF_{1α}.

© 2010 Elsevier Ltd. All rights reserved.

Unmet therapeutic needs in the treatment of inflammation and arthritis include the need for improved analgesic activity and disease modification relative to current COX-2 inhibition therapies. In particular, analgesic agents that display increased maximal inhibition of pain or utility in a broader population would provide benefit to aging patients. Development of a new generation of anti-inflammatory drug with better efficacy through an alternative mechanism providing a different biochemical profile is a very urgent and challenging mission for drug discovery scientists.

It has been well established that prostaglandin E₂ (PGE₂) is an important mediator in acute and chronic inflammation.¹ Reduction of PGE₂ production by the inhibition of COX-2 can remit the signs and symptoms of pain and edema associated with inflammation. Microsomal prostaglandin synthase type 1 (mPGES-1) is a member of the MAPEG family of glutathione transferases, which also includes FLAP and LTC₄ synthase. mPGES-1 is downstream of COX-2 in the arachidonic acid pathway. It is up-regulated in response to inflammatory signals and is primarily responsible for the generation of PGE₂ during inflammation. Murine knockout of mPGES-1 demonstrates almost complete reduction of PGE₂ from peritoneal macrophages stimulated with LPS and complete reversal of the severity and incidence in collagen induced arthritis.² Therefore, a selective inhibitor of mPGES-1 would be expected to inhibit PGE₂ production induced by inflammation while sparing constitutive PGE₂, prostacyclin (PGI₂), and thromboxane production. This selectivity should differentiate mPGES-1 inhibitors from NSAIDs and COX-2 inhibitors in the treatment of inflammation and arthritis.³

Abbreviations: PG, prostaglandin; COX, cyclooxygenase; NSAID, nonsteroidal anti-inflammatory drug; mPGES-1, microsomal prostaglandin E synthase-1; PGE₂, prostaglandin E₂; PGI₂, prostaglandin I₂; PGF_{2α}, prostaglandin F_{2α}; 6-keto PGF_{1α}, 6-keto prostaglandin F_{1α}.

* Corresponding author. Tel.: +1 636 527 5037; fax: +1 636 247 2086.

E-mail addresses: jl47wang@yahoo.com, jane.1.wang@pfizer.com (J. Wang).

Interest in mPGES-1 as a new therapeutic target is growing and the number of publications, patent applications, and conference presentations have increased recently. There are several reported small molecule mPGES-1 inhibitors in the literature (Fig. 1). MK-886 (**1**),⁴ a FLAP inhibitor with an indole core, displayed mPGES-1 inhibition for rat (IC₅₀ = 3.2 μM) and human (IC₅₀ = 1.6 μM), but it also possessed potent FLAP inhibition (IC₅₀ = 0.026–0.1 μM). Merck scientists have carried out SAR studies and produced more potent and selective mPGES-1 inhibitors (**2**).⁴ Due to high protein binding and poor cell permeability, the IC₅₀ of **2** in the cell assay was right shifted and it did not display reasonable cell activity. Biopix also published a series of patents covering mPGES-1 inhibitors which were based on an indole scaffold (**3**).⁵ These compounds were claimed as potent mPGES-1 inhibitors (IC₅₀ = 0.062–0.075 μM), but no cellular or in vivo data were reported. Merck disclosed another series of mPGES-1 inhibitors (**4**) derived from a JAK inhibitor,^{6a} which displayed sub nanomolar potency (IC₅₀ = 0.001 μM),^{6b} and more than 1000-fold selectivity over other prostaglandin synthases. In the A549 cells with 50% FBS, it displayed an IC₅₀ = 0.42 μM. Biopix described other non-indole mPGES-1 inhibitors but they lacked low nanomolar potency (**5**^{7a} IC₅₀ = 0.39 μM; **6**^{7b} IC₅₀ = 1.3 μM; **7**^{7c} IC₅₀ = 1.1 μM). More recently, Merck reported diarylimidazole **8**⁸ as a potent mPGES-1 inhibitor (IC₅₀ = 0.0008 μM no other data reported). Koeberle et al. had published a series of pirinixic acid derivatives^{8b} and the benzo[g]indole-3-carboxylate series^{8c} as novel mPGES-1/5-LO dual inhibitors with valuable pharmacological profile.

A series of benzo-thiopyran S-dioxides, exemplified by **9** (Fig. 2) were discovered by high throughput screening of the Pfizer chemical file against the human mPGES-1 enzyme. This series of compounds demonstrated moderate inhibition against human mPGES-1⁹ (IC₅₀ = 1.68 μM) and displayed selectivity for mPGES-1 (PGE₂) over COX-2 (PGF_{2α}) in the IL-1-stimulated fetal fibroblast cell assay¹⁰ (PGE₂ IC₅₀ = 3.4 μM; PGF_{2α} IC₅₀ >90 μM). PGF_{2α} was generated as a

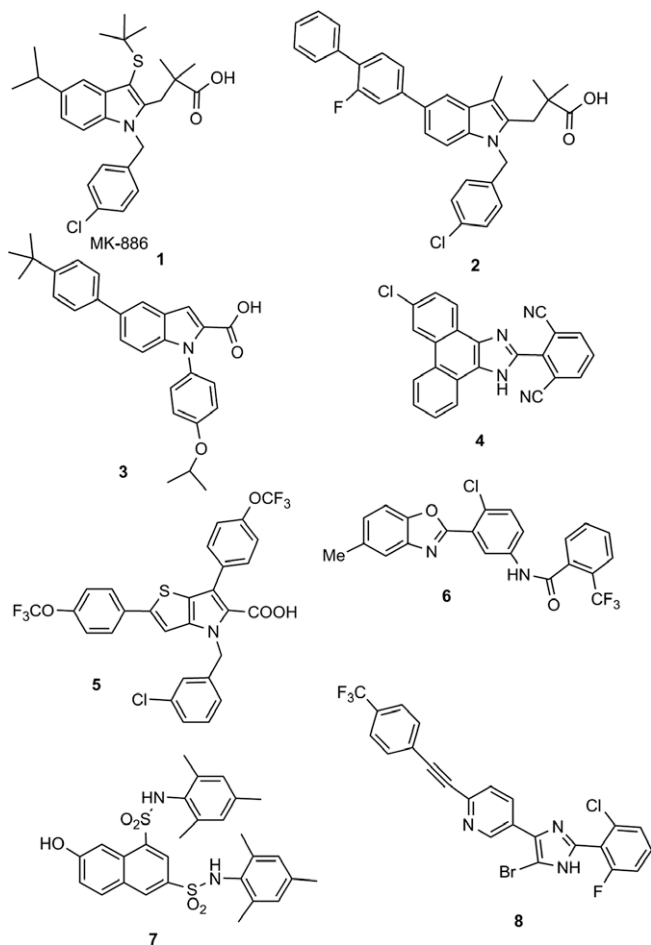


Figure 1. Structures of mPGES-1 inhibitors.

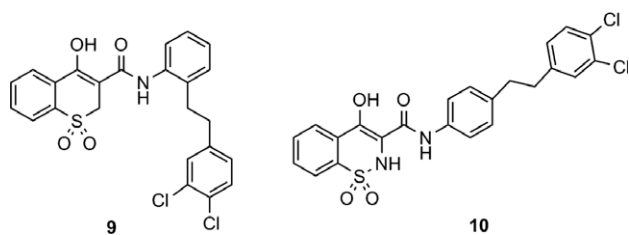
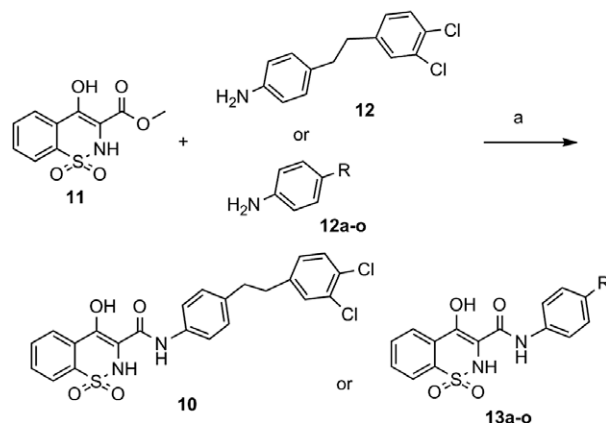


Figure 2. Structures of early leads.

stable product of PGH_2 as described by Mbalaviele et al.^{10b} We explored further to replace the benzo-thiopyran with dioxobenzo-thiazinone (oxicam type) to produce compound **10**. We realized that since oxicams were COX-1 and COX-2 inhibitors, we wanted to make sure that they were truly mPGES-1 inhibitors and not COX inhibitors by screening them in our COX assays. None of these oxicam analogs had COX-1 or COX-2 inhibition less than 50 μM (data not shown).

As described in Scheme 1,¹¹ compound **10** can be prepared by heating 4-(3,4-dichlorophenylethyl) aniline **12**¹² with commercially available methyl 4-hydroxy-2H-1,2-benzothiazine-3-carboxylate 1,1-dioxide **11**. Compound **10** demonstrated potency both in the enzyme (mPGES-1 IC_{50} = 0.11 μM) and cell-based assays (PGE₂ IC_{50} = 0.46 μM), and it demonstrated selectivity for mPGES-1 over COX-2 (PGF_{2 α} IC_{50} > 68 μM). The selectivity over COX-2 in cellular assay was confirmed using recombinant enzyme assays (hCOX-1 IC_{50} = 489 μM , hCOX-2 IC_{50} = 467 μM). Based on this data, we conducted an extensive SAR exploration on the four rings (A, B, C, and

Scheme 1. Reagents and conditions: (a) *o*-xylene, 135 °C, pyridine, 4 Å molecular sieves, overnight, yield depending on the aniline used.

D), the linker (X), and the linker position on the C ring (see Fig. 3 for a general structure).

Our initial effort was to evaluate whether we could replace the two carbon linker (X) (analog **10**) with no linker between the C and D rings and reduced the 3,4-dichloro to 4-chloro (**13a**). Biphenyl **13a** was prepared by utilizing the chemistry described in Scheme 1 by heating aniline (**12a**) with ester **11** in *o*-xylene. Biphenyl **13a** exhibited threefold less potency both in the enzyme and cell assay compared with compound **10**, but it kept a similar cell to enzyme right shift ratio (threefold). Based on this data, we designed analogs with a one hetero atom linker using a nitrogen, an oxygen, or a ketone (**13b–e**) to explore the impact of these atoms to mPGES-1 inhibition. These analogs were prepared by utilizing the chemistry described in Scheme 1 by heating various anilines (**12b–e**) with ester **11** in *o*-xylene. The phenoxy **13b** demonstrated a twofold decrease enzyme inhibition and a 4.6-fold decrease in cell potency compared with **13a**. The aniline **13c** exhibited a twofold improvement in enzyme potency, but it showed a twofold decrease potency in the cell compared with **13a**. The *para* substituted keto analog **13d** had similar cell potency compared with **13a**, but the *meta* substituted keto **13e** had greatly decreased mPGES-1 inhibition. This data suggests that human mPGES-1 enzyme inhibition is not very sensitive to the linker length or the nature of the heteroatoms, both H-bond donors and acceptors had comparable potency against mPGES-1. Enzyme activity varied within a ± 2 -fold range, when the C and D rings were linked at the *para* position. We observed that incorporation of a heteroatom linker has a greater effect on the cellular activity and ratio of the cellular activity to enzyme activity varied fivefold (biphenyl **13a**), 10-fold (keto **13d**), 13-fold (phenoxy **13b**), and 28-fold (aniline **13c**). This was possibly due to the hydrogen bond donor nature of the aniline, which decreased cell penetration. This data also demonstrated that the position of the D ring on the C ring was very critical for the mPGES-1 inhibition (Table 1).

Since **13a** demonstrated good PGE₂ inhibition both in the enzyme and cell and displayed favorable $c \log P^{13a}$ (4.59) and $c \log D^{13b}$ (0.710) compared with **10** ($c \log P$ = 5.69 and $c \log D$ = 1.70). We sought to further improve the potency and selectivity by varying the substituents on the D ring of the biphenyl analog (**13a**) to boost

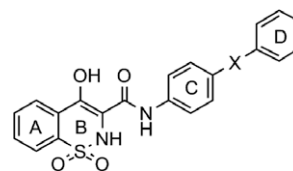
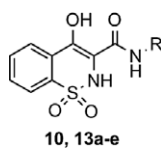


Figure 3. General structure.

Table 1

SAR of mPGES-1 inhibition by variation of the linker between the C and D rings, compounds **10**, **13a** to **13e**



#	Structure R	mPGES-1 IC ₅₀ μM ^a	Cell IC ₅₀ μM ^b PGE ₂ /PGF _{2α}	mPGES-1/ COX-2 selectivity
13a		0.29	1.45/33.7	23
13b		0.53	6.73/70	10
13c		0.15	4.24/>100	>23
13d		0.11	1.14/95.6	84
13e		3.91	2.16/95.3	44

^a For enzyme assay conditions, see Ref. 9. The IC₅₀ curve was generated based on duplicated data, which was done $n \geq 2$ except **13a** $n = 1$.

^b For cellular assay conditions, see Ref. 10. The IC₅₀ curve was generated based on duplicated data, which was done $n = 1$.

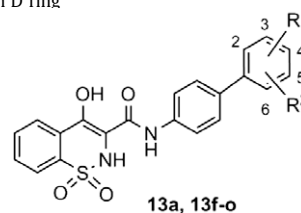
its potency. We used the same chemistry described in Scheme 1 to conduct the SAR exploration.

After evaluation of various substituents, we observed that the nature of the substituents and group positions on the D ring were important to their mPGES-1 inhibition, (see examples in Table 2). In general, *para* chloro (**13a**) was more potent than *meta* chloro (**13f**) on the D ring, disubstituted analogs (**13j**, **13k**, **13l**, **13m**) are more potent mPGES-1 inhibitors than mono substituted analogs (**13a**, **13f**, **13g**). Analog (**13j**) with 3,4-dichloro was more preferred than that with 2,3-dichloro (**13k**) and 2,4-dichloro (**13l**). Chloro (**13a**) and methyl (**13g**) substituents were much more preferred than hydrogen (**13i**), cyano (**13h**), and methoxy (**13o**) substituents. Analog **13j** demonstrated the greatest inhibition both in the human mPGES-1 enzyme assay and cell-based assay against PGE₂ production, but did not exhibit any COX inhibition (hCOX-1 IC₅₀ = 118 μM, hCOX-2 IC₅₀ = 263 μM). It also displayed over 238-fold selectivity for COX-2 in the cell.

With demonstration of low nanomolar potency both in the enzyme and cell assays and selectivity for COX-2, we sought to incorporate a pyridyl ring as replacement for either the C or D phenyl ring to further decrease $\log P$ of **13j** (5.2). Analogs **17** and **18** were prepared by the chemistry described in Scheme 2 via a Suzuki reaction¹⁴ to form the dichloro-phenylpyridine amine **16a** and chloro-pyridinylaniline **16b**, which were then heated with ester **11** in xylene to provide the desired products **17** and **18**. Analogs **19** and **20** were prepared by alternative chemistry (Scheme 3), since applying the normal chemistry as in Scheme 2 did not lead to the desired products with the pyridin-2-amine. We used the same Suzuki reaction to prepare the dichlorophenylpyridine amines (**23a–b**), followed by reacting with known starting material **24** to form the amides¹⁵ (**25** and **26**). Analogs **19** and **20**¹⁶ were

Table 2

SAR of substituents on D ring

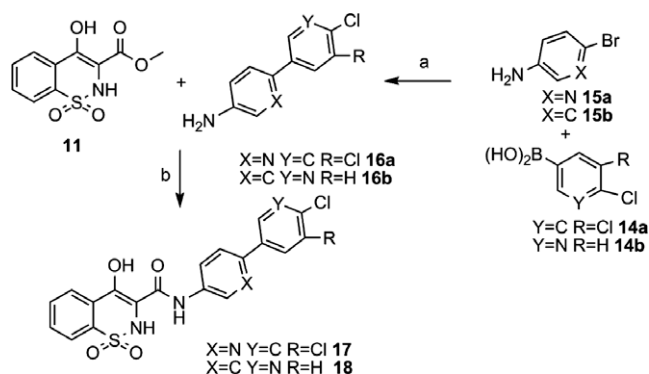


#	Structure R ¹ and R ²	mPGES-1 IC ₅₀ μM ^a	Cell IC ₅₀ μM ^b PGE ₂ /PGF _{2α}	mPGES-1/COX-2 selectivity
13a	R ¹ = H R ² = 4-Cl	0.29	1.45/33.7	23
13f	R ¹ = H R ² = 3-Cl	0.86	3.44/74.7	22
13g	R ¹ = H R ² = 4-Me	<0.07	2.24/>100	>45
13h	R ¹ = H R ² = 4-CN	3.96	n.d.	n.d.
13i	R ¹ = H R ² = 4-H	3.13	6.73/92.6	14
13j	R ¹ = 3-Cl R ² = 4-Cl	0.016	0.42/>100	>238
13k	R ¹ = 2-Cl R ² = 3-Cl	0.038	<0.92/44.4	>48
13l	R ¹ = 2-Cl R ² = 4-Cl	0.043	<0.76/>74.8	>98
13m	R ¹ = 3-Me R ² = 4-Me	<0.026	<0.75/>57.7	>77
13n	R ¹ = 2-Me R ² = 3-Me	1.00	6.59/94.7	14
13o	R ¹ = 3-OMe R ² = 4-OMe	32.2	n.d.	n.d.

n.d.: no data was provided.

^a The IC₅₀ curve was generated based on duplicated data, which was done $n \geq 2$ except **13a**, **13g**, and **13o** $n = 1$.

^b The IC₅₀ curve was generated based on duplicated data, which was done $n \geq 5$ for **13j** and **13m**, $n = 3$ for **13f**, **13k**, and **13i**, and $n = 1$ for **13a**, **13g**, **13l**, and **13n**.

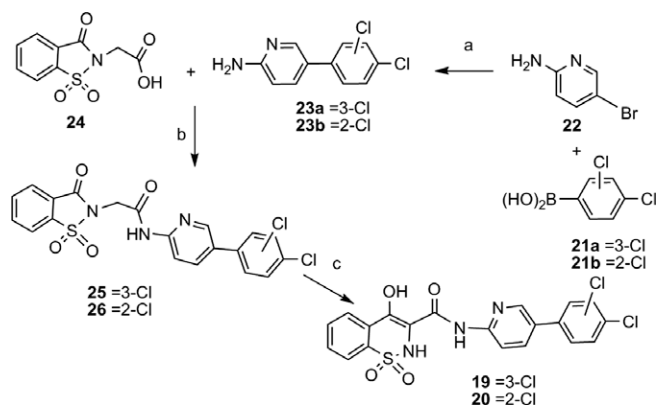


Scheme 2. Reagents and conditions: (a) toluene/water/ethanol = 4:2:1, 3 equiv Na₂CO₃, Pd(PPh₃)₄, 85 °C, overnight, yield 50%; (b) *o*-xylene, 135 °C, pyridine, 4 Å molecular sieves, overnight, yield 39% and 43%.

obtained after treating the amides (**25** and **26**) with lithium *i*-propoxide in DMSO.

Analog bearing pyridyl in the C or D ring (**18**, **19**, and **20**) exhibited a dramatic decrease in activity, except the 3-pyridyl analog **17** which uniquely retained mPGES-1 activity in both enzyme and cell assays (Table 3). This data suggested that the biphenyl group was more preferred for mPGES-1 activity (Table 4).

As incorporation of polar functionality in the C and D rings led to a decrease in activity, next we wanted to introduce polar groups in the A ring and to identify a conformationally less constrained B ring to increase aqueous solubility. First, we incorporated methoxy

**Table 3**

SAR of pyridine as either C or D ring

#	Structure R	mPGES-1 ^a IC ₅₀ (μM)	Cell IC ₅₀ ^b (μM) PGE ₂ /PGF _{2α}	c log P
17		0.16	0.69/33.7	4.71
18		12.7	n.d.	3.30
19		65.6	n.d.	4.50
20		11.7	n.d.	4.37

^a The IC₅₀ curve was generated based on duplicated data, which was done $n = 1$ except 17 $n = 4$.^b The IC₅₀ curve was generated based on duplicated data, which was done $n = 2$.

or hydroxyl groups into the A ring. Compounds (**30** and **32**) were prepared (Scheme 4) by heating aniline **12j** with esters **27** and **28**, and compound **30** and **32** were O-demethylated to form compounds **31** and **33**. The *N*-methyl analog **34** (Scheme 4) was also prepared by a one step reaction via heating aniline **12j** and **29** in xylene. The B ring saturated analog **36** was obtained (Scheme 5) by first hydrogenation of ester **11** under 10% Pd on carbon conditions, followed by hydrolysis to form **35**. Then **35** was reacted with aniline **12j** to form amide **36** using the same amide formation condition described in Scheme 3. The B-ring opened analogs **38** and **39** (Scheme 6) were prepared by first forming amide **37**, which then was treated with sodium hydroxide to form desired product **38**.

Table 4

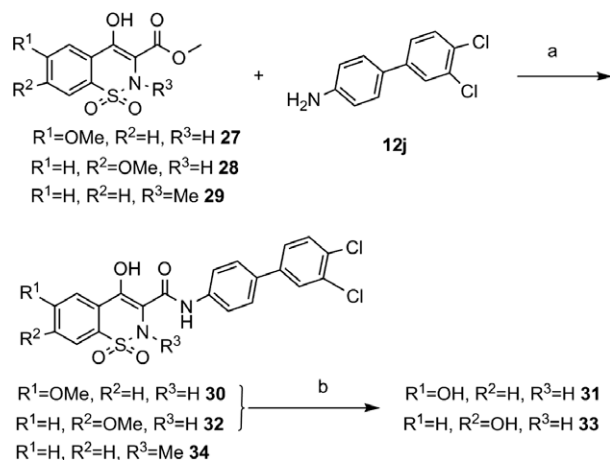
A and B rings effect on mPGES-1 inhibition

#	Structure R	mPGES-1 IC ₅₀ ^a (μM)	Cell IC ₅₀ ^b (μM) PGE ₂ /PGF _{2α}	mPGES-1/COX-2 selectivity
30		0.69	1.29/>100	>77
31		0.098	1.45/>100	>69
32		3.05	n.d.	n.d.
33		0.18	n.d.	n.d.
34		0.28	2.04/n.d.	n.d.
36		0.19	0.67/>100	>149
38		5.76	37.6/>100	>3
39		29.6	n.d.	n.d.

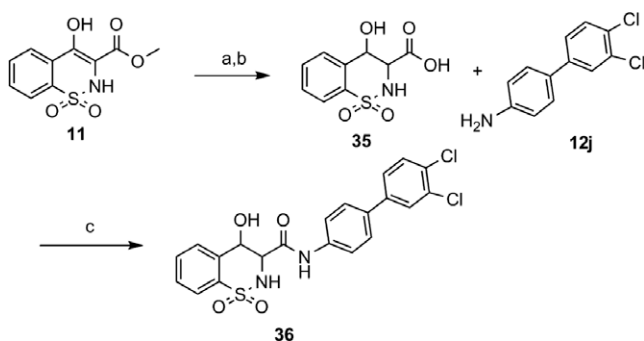
^a The IC₅₀ curve was generated based on duplicated data, which was done $n \geq 2$ except **39** $n = 1$.^b The IC₅₀ curve was generated based on duplicated data, which was done $n \geq 2$ except **31**, **34**, and **38** $n = 1$.

Carboxylic acid **38** was reduced by treating with borane–THF to obtain alcohol **39** as a minor product.

The analogs with substituents on the A ring (**30**, **31**, **32**, and **33**) did not display improved the mPGES-1 inhibition. For analogs **30** and **32**, both having a methoxy group on the A ring, lost activity, 42-fold (**30**) and 185-fold (**32**), respectively. With hydroxyl replacing methoxy on the A ring (**31** and **33**), they displayed better activity compared with **30** and **32**, and only lost sixfold and 11-fold activity compared with **13j**. It seemed that position 6 (**30** and **31**) had better toleration than position 7 (**32** and **33**), and the hydroxyl group (**31** and **33**) was a more preferred group than methoxy (**30** and **32**). Methylated sulfonamide **34** was designed to disrupt the ring planarity to improve the solubility, but it lost 17-fold mPGES-1 inhibition in enzyme and fivefold inhibition in the cell



Scheme 4. Reagents and conditions: (a) *o*-xylene, 135 °C, pyridine, 44 Å molecule sieves, overnight, yield depending on the anilines; (b) 5.0 equiv BBr₃, dichloroethane, 60 °C for 2 h, yield 50%.

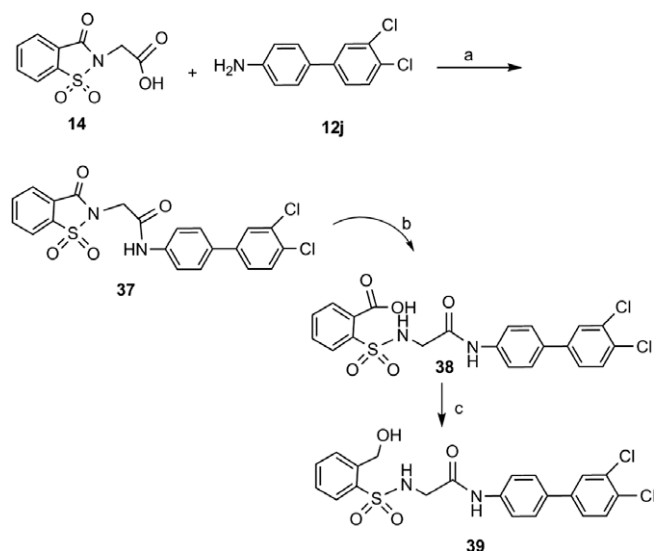


Scheme 5. Reagents and conditions: (a) EtOAc, cat. AcOH, 10% Pd–C, H₂ 45 psi, overnight, yield 90%; (b) THF/MeOH = 4:1, 4 equiv NaOH (2.5 N), 50 °C, 2 h, 1 N HCl, yield 100%; (c) 2.4 equiv tributylamine, 1.2 equiv 2-chloro-1-methylpyridinium iodide, dichloromethane, reflux for 1 h, yield 87%.

and had same aqueous solubility range as **13j** (<3 μM). Although the saturated B-ring analog **36** had a better *c log P* (4.14) and improved water solubility¹⁷ from 3 μM (**13j**) to 25 μM, it exhibited a 10-fold decreased enzyme inhibition and 1.5-fold decrease in the cell. Analog **36** demonstrated no COX inhibition in the enzyme assay (hCOX-1 IC₅₀ >50 μM, hCOX-2 IC₅₀ >50 μM). We determined that the acidic proton within the dioxobenzothiazinone is very important to achieve potent mPGES-1 inhibition. In order to improve solubility and further lower the *c log P*, we opened the B (thiazinone) ring to provide carboxylic acid **38** and alcohol **39** to mimic the oxicam. Unfortunately, analogs **38** and **39** were poor mPGES-1 inhibitors.

Because **13j** displayed excellent potency for mPGES-1 and selectivity over COX-2, we wanted to check whether **13j** had inhibitory effects on other prostanoids, such as thromboxane B₂ (TXB₂) and 6-keto-PGF_{1α}. The inducible nature of mPGES-1 and COX-2 expression made synovial fibroblasts derived from patients with rheumatoid arthritis (RASf) the suitable cells for the search of inhibitors that selectively inhibit mPGES-1 function in converting PGH₂ to PGE₂.^{10b} **13j** blocked the production of PGE₂ from PGH₂ (PGE₂ IC₅₀ ~0.5 μM), while sparing the production of 6-keto PGF_{1α} (a metabolite of PGI₂), PGF_{2α}, and TXB₂ (all three IC₅₀ >100 μM).

In summary, we have identified very potent and selective mPGES-1 inhibitors which demonstrated better cell activity over previously reported series. Compound **13j** displayed excellent mPGES-1 inhibition and selectivity over COX-2 in the human fetal fibroblast cell assay. In addition, the selectivity of **13j** over other



Scheme 6. Reagents and conditions: (a) 2.4 equiv tributylamine, 1.2 equiv 2-chloro-1-methylpyridinium iodide, dichloromethane, reflux for 1 h, yield 75%; (b) THF/MeOH = 4:1, 5 equiv NaOH (2.5 N), rt, 4 h, 1 N HCl, yield 100%; (c) THF, 4 equiv BH₃·THF, room temp, 3 h, added water, 50 °C, 0.5 h, yield 10%.

prostanoids was further demonstrated in IL-1β-stimulated RASf cells.¹⁸ It also inhibited PGE₂ production in the LPS/human whole blood assay¹⁹ with an IC₅₀ around 5 μM. The low inhibition in the whole blood assay was likely due to the high protein binding of the molecule.

Supplementary data

Supplementary data associated with this article can be found, in the online version, at doi:10.1016/j.bmcl.2010.01.060.

References and notes

- Kobayashi, T.; Narumiya, S. *Prostagland. Other Lipid Mediat.* **2002**, 68–69, 557.
- Trebino, C.; Stock, J.; Gibbons, C.; Naiman, B.; Wachtmann, T.; Umland, J.; Pandher, K.; Lapointe, J.; Saha, S.; Roach, M.; Carter, D.; Thomas, N.; Durtschi, B.; McNeish, J.; Hambor, J.; Jakobsson, P.; Carty, T.; Perez, J.; Audoly, L. *Proc. Natl. Acad. Sci. U.S.A.* **2003**, 100, 9044.
- (a) Portanova, J. P.; Zhang, Y.; Anderson, G.; Hauser, S.; Masferrer, J.; Seibert, K.; Gregory, S.; Isakson, P. *J. Exp. Med.* **1996**, 184, 883; (b) Pulichino, A. M.; Rowland, S.; Wu, T.; Clark, P.; Xu, D.; Mathieu, M.; Riendeau, D.; Audoly, L., et al. *J. Pharmacol. Exp. Ther.* **2006**, 319, 1043; (c) Murata, T.; Ushikubi, F.; Matsuoka, T.; Hirata, M.; Yamasaki, A.; Sugimoto, Y.; Ichikawa, A.; Aze, Y.; Tanaka, T.; Yoshida, N.; Ueno, A.; Oh-ishi, S.; Narumiya, S. *Nature* **1997**, 388, 678; (d) Jakobsson, P. J.; Thoren, S.; Morgenstern, R.; Samuelsson, B. *Proc. Natl. Acad. Sci. U.S.A.* **1999**, 96, 7220; (e) Murakami, M.; Naraba, H.; Tanioka, T.; Semmyo, N.; Nakatani, Y.; Kojima, F.; Ikeda, T.; Fueki, M.; Ueno, A.; Oh, S.; Kudo, I. *J. Biol. Chem.* **2000**, 275, 32783; (f) Murakami, M.; Kudo, I. *Prog. Lipid. Res.* **2004**, 43, 3.
- Riendeau, D.; Aspiotis, R.; Eithier, D.; Gareau, Y.; Grimma, E.; Guaya, J.; Guirala, S.; Juteau, J.; Mancina, H.; Méthota, N.; Rubina, J.; Friesena, R. *Bioorg. Med. Chem. Lett.* **2005**, 15, 3352.
- Olofsson, K.; Suna, E.; Pelcman, B.; Ozola, V.; Katkevics, M.; Kalvins, I. *Indoles Useful in the Treatment of Inflammation*. WO 2005/123673 A1, 2005.
- (a) Chau, A.; Côté, B.; Ducharme, Y.; Frenette, R.; Friesen, R. W.; Gagnon, M.; Giroux, A.; Martins, E.; Yu, H.; Wu, T. 2-(Phenyl or heterocyclic)-1*H*-phenanthro[9,10-*D*]imidazoles as mPGES-1 inhibitors. WO 063466 A1, 2006; (b) Côté, B.; Boulet, L.; Brideau, C.; Claveau, D.; Ethier, D.; Frenette, R.; Gagnon, M.; Giroux, A.; Guay, J.; Guiral, S.; Mancini, J.; Martins, E.; Massé, F.; Méthot, N.; Riendeau, D.; Rubin, J.; Xu, D.; Yu, H.; Ducharme, Y.; Friesen, R. *Bioorg. Med. Chem. Lett.* **2007**, 17, 6816.
- (a) Pelcman, B.; Olofsson, K.; Arsenjans, P.; Ozola, V.; Suna, E.; Kalvins, I. *Thienopyrroles Useful in the Treatment of Inflammation*. WO Patent 077412 A1, 2006; (b) Pelcman, B.; Olofsson, K.; Schaal, W.; Kalvins, I.; Katkevics, M.; Ozola, V.; Suna, E. *Benzoxazoles Useful in the Treatment of Inflammation*. WO 2007/042816 A1, 2007; (c) Pelcman, B.; Olofsson, K.; Habarova, O.; Kalvins, I.; Suna, E.; Trapencieris, P.; Andrianov, V. *Naphthalene-disulfonamides Useful for the Treatment of Inflammation*. WO 2007/042817 A1, 2007.
- (a) Juteau, H.; Wu, T.; Ducharme, Y. In *234th National Meeting of the Am. Chem. Soc.* Boston, MA, August, 2007; MEDI 430; (b) Koeberle, A.; Zettl, H.; Greiner, C.; Wurglics, M.; Schubert-Zsilavecz, M.; Werz, O. *J. Med. Chem.* **2008**, 51, 8068;

- (c) Koeberle, A.; Haberl, E.; Rossi, A.; Pergola, C.; Dehm, F.; Northoff, H.; Troschuetz, R.; Sautebin, L.; Werz, O. *Bioorg. Med. Chem.* **2009**, *17*, 7924.
9. Incubation of enzyme with 2 μM PGH_2 for 41 s at rt and assessment of PGE_2 by ELISA. Enzyme is suspended in 100 mM K_3PO_4 at pH 6.2 buffer and 2.5 mM glutathione. Compound solubilized in DMSO and added at a 1:9 w/w DMSO to enzyme ratio. PGH_2 (Cayman Chemical, Ann Arbor MI) is diluted 12.8 \times in ice cold 10 mM HCl from a 278 μM stock in acetone. The reaction is begun by the addition of 1:10 volume of PGH_2 to the enzyme inhibitor mixture for a final concentration of 2 μM . The reaction is terminated by the addition of 1:10 volumes of 2.5 mM FeCl_2 . The reaction is immediately diluted 120 \times into ELISA buffer (according to Cayman Chemical, Ann Arbor MI recipe). PGE_2 formed was calculated from a standard curve of PGE_2 by ELISA (Cayman Chemical, Ann Arbor MI). The % control activity was calculated as the percentage difference between negative control (100% inhibited with a reference compound) and enzyme only control. The difference between enzymatic versus non-enzymatic production of PGE_2 are typically 3–4-fold. IC_{50} 's are calculated by 4 parameter log fit of the % control data.
 10. (a) Human fetal fibroblasts (FF), plated at 3×10^6 cells/ cm^2 in DMEM supplemented with 15% FBS, glutamine, pen/strep and HEPES, were incubated at 37 °C, 5% CO_2 . Approximately 20–24 h later, media were refreshed and cells were treated with 1 ng/mL IL-1 β for an additional 20–24 h, after which they were washed once with DMEM without serum. Cells were then incubated with compounds for 50 min in DMEM without serum then with 10 μM arachidonic acid for 10 min. PGE_2 levels were analyzed by ELISA. To measure $\text{PGF}_{2\alpha}$ levels, FF were processed as described above, except that after incubation with the compounds for 50 min, cells were treated with SnCl_2 (which converts PGH_2 non-enzymatically to $\text{PGF}_{2\alpha}$) for 10 min before treatment with 10 μM arachidonic acid for an additional 10 min. In this assay, a COX-2 inhibitor blocks the production of PGH_2 and consequently neither PGE_2 nor $\text{PGF}_{2\alpha}$ is synthesized, whereas PGE_2 not $\text{PGF}_{2\alpha}$ production should be inhibited by a mPGES-1 inhibitor. $\text{PGF}_{2\alpha}$ levels were analyzed by ELISA; (b) Mbalaviele, G.; Pauleya, A.; Shaffera, A.; Zweifela, B.; Mathialagana, S.; Mnicha, S.; Nemirovskiya, O.; Cartera, J.; Giersea, J.; Wang, J.; Vazquez, M.; Moore, W.; Masferrer, J. *Biochem. Pharmacol.*, pending.
 11. Zia-ur-Rehman, M.; Choudary, J. A.; Ahmad, S.; Siddiqui, H. L. *Chem. Pharm. Bull.* **2006**, *54*, 1175.
 12. Simons, L. J.; Caprathe, B. W.; Callahan, M., et al *Bioorg. Med. Chem. Lett.* **2009**, *19*, 654.
 13. (a) This protocol uses the BioByte (www.biobyte.com) program c log P, version 4.3, to calculate the logarithm of the partition coefficient. The partition coefficient, often taken on the log scale (log P) is defined for neutral compounds. The reference system is octanol/water. To take ionization into account distribution coefficients (log D) can be calculated at a selected pH, for example, 7.4 or 6.5. Often log D values have more physiological meaning than log P values; (b) Calculated logarithm of the octanol/water distribution coefficient using ACD pchbat version 9.3. PH (default value = 7.4) IONIZE (default value = UnSet).
 14. Shen, H. C.; Ding, F.; Luell, S.; Forrest, M.; Carballo-Jane, E.; Wu, K.; Wu, T.; Cheng, K.; Wilsie, L.; Krsmanovic, M.; Taggart, A.; Ren, N.; Cai, T.; Deng, Q.; Chen, Q.; Wang, J.; Wolff, M.; Tong, X.; Holt, T.; Waters, G.; Hammond, M.; Tata, J.; Colletti, S. *J. Med. Chem.* **2007**, *50*, 6303.
 15. Groundwater, P. W.; Garnett, I.; Morton, A. J. *J. Chem. Soc., Perkin Trans. 1* **2001**, 2781.
 16. Herrmann, W.; Geibei, W.; Satzinger, G. DE 3,212,485 A1, 1983.
 17. An aqueous solution (with 2% DMSO) of the test compound is stirred for 24 h at room temperature, then filtered. The nitrogen content of the filtered aqueous solution is measured and, in conjunction with the molecular formula, is used to calculate the concentration of the solution. True thermodynamic solubility requires the measurement of the concentration of saturated aqueous solutions in equilibrium with solid; these measurements are usually laborious and relatively expensive. This apparent solubility assay is a high-throughput, relatively low cost test. Data published by Analiza (see their website: <http://www.analiza.com>) show a good correlation between data from this high-throughput assay and traditional shake flask solubility data ($r^2 = 0.9993$, with standard deviation of <3%). Method: A Hamilton Starlet Liquid Handler or Analiza's ADW (Automated Discovery Workstation) robotic platform was used for all steps of the analysis. 50 mM sodium phosphate buffer, at the indicated pH, was freshly prepared from NaH_2PO_4 and Na_2HPO_4 and filtered. Buffer (294 μL) was combined with 6 μL of 30 mM DMSO stock solutions in a Millipore polycarbonate filter solubility plate (part# MSSLBPC10) for a final a final DMSO concentration of 2%. The plates were heat sealed with a polypropylene seal. After 24 h of 200 rpm shaking at room temperature (23–25 °C), the plates were vacuum filtered into deep well receiver plates. Filtrates were injected into the chemiluminescent nitrogen detector (Antek 8060) for quantification. Apparent concentration was divided by the number of nitrogens in the sample (from the molecular formula) to determine the concentration. The results are reported here in $\mu\text{g/mL}$ and μM .
 18. Synovial fibroblasts derived from patients with rheumatoid arthritis (RASf), were isolated via enzymatic digestions from primary synovial tissues isolated after knee synovectomy as previously described. RASf were plated at 8×10^4 cells/ cm^2 and cultured for three days in DMEM containing 10 μM L-glutamine, 25 μM HEPES, 10 units/mL penicillin, 10 $\mu\text{g/mL}$ streptomycin, supplemented with 10% (v/v) fetal bovine serum (FBS), at 37 °C in 95% air, 5% CO_2 atmosphere. To test the effects of the inhibitors on prostaglandin (PG) production during 24 h incubation, the culture media were replaced with fresh DMEM containing 1% (v/v) FBS, and cells were treated for 24 h with 1 ng/mL IL-1 β in the presence of vehicle (1% Me_2SO , final concentration) or the inhibitors (1% Me_2SO , final concentration). The conditioned media were then collected for PG analysis. To determine direct effects of the inhibitors on enzyme activity, cells were treated for 24 h with 1 ng/mL IL-1 β as described above. The conditioned media were removed, and cells were washed twice with serum-free media. Cells were then treated with the media containing either the vehicle (1% Me_2SO) or the inhibitors (1% Me_2SO) for 50 min, and with 10 μM arachidonic acid for additional 10 min, at 37 °C in 95% air, 5% CO_2 atmosphere, and the conditioned media were collected for PG analysis. For $\text{PGF}_{2\alpha}$ studies, 2 mg/mL SnCl_2 was added to the cells 40 min after addition of the inhibitors (or 10 min before the addition of arachidonic acid). The levels of PGE_2 , $\text{PGF}_{1\alpha}$ and $\text{PGF}_{2\alpha}$ in the conditioned media were measured by ELISA.
 19. Human whole blood collected from healthy human donors in heparinized tubes was mixed with human head and neck squamous cell carcinoma, 1483 cells. Briefly, 100 μL blood/well (384-well) were mixed with 10^5 1483 cells/well and incubated with the compounds for 15 min at 37 °C in 95% air, 5% CO_2 atmosphere, then with 30 μM arachidonic acid for 10 min. The assay plates were centrifuged at 930g for 10 min at room temperature, and the plasma was removed for quantitation of PGE_2 levels by ELISA.